Histol Histopathol (2017) 32: 899-907

http://www.hh.um.es

Histology and Histopathology

From Cell Biology to Tissue Engineering

Targeting miR-155 suppresses proliferation and induces apoptosis of HL-60 cells by targeting Slug/PUMA signal

Hui Liang[1], Ziyan Dong[2], Jiang-Feng Liu[1], Wei Chuang[2], Li-Zhen Gao[4] and Yu-Guo Ren[3]

[1]Department of Hematology, Qingdao women and children's Hospital, Qingdao, [2]Department of Ophthalmology and Otorhinolaryngology, People's Hospital of Lanshan District, Rizhao, [3]Clinical Laboratory, People's Hospital of Laiwu, Laiwu and [4]Clinical Laboratory, People's Hospital of Zhangqiu, Jinan, Shandong, China

Summary. Recent studies have shown that high miR-155 expression was associated with poor prognosis in patients with acute myelogeneous leukemia (AML). Furthermore, targeting miR-155 results in monocytic differentiation and apoptosis. However, the exact role and mechanisms of miR-155 in human AML remains speculative. HL-60 cells were treated with anti-miR-155 for 72 h. Cell growth and apoptosis in vitro were detected by MTT, BrdU proliferation, colony formation and flow cytometry assay. The effect of anti-miR-155 on growth of HL-60 cells was also evaluated in a leukemia mouse model. Slug cDNA and PUMA siRNA trannsfection was used to assess the signal pathway. Different protein expression was detected by western blot assay and quantitative reverse transcriptase polymerase chain reaction (qRT-PCR) assay. The results shown that targeting miR-155 resulted in a 24-fold decrease of miR-155 expression compared to negative control in the HL-60 cells. Targeting miR-155 significantly downregulated Slug and upregulated PUMA expression, and decreased HL-60 cell growth by 70% , impaired colony formation by approximately 60%, and increased HL-60 cell apoptosis by 45%. Targeting PUMA reversed miR-155 sliencing-induced proliferation and apoptosis of HL-60 cells. Restoration of Slug decreased PUMA expression. In murine engraftment models of HL-60 cells, we showed that targeting miR-155 was able to reduce tumor growth. This was accompanied with decreased Slug expression and increased PUMA expression in these tumors. Collectively, our findings strongly suggest targeting miR-155 exhibited *in vivo* and *in vitro* antileukemic activities in AML through a novel mechanism resulting in inhibition of *Slug* expression and increase of PUMA expression.

Key words: Acute myeloid leukemia, miR-155, Slug, PUMA, Apoptosis

Offprint requests to: Dr. Hui Liang, Department of Hematology, Qingdao Women and Children's Hospital, Qingdao, 266005, China. e-mail: blooddoc@126.com

DOI: 10.14670/HH-11-837

Introduction

Leukemia is a cancer which arises from uncontrolled proliferation in the hematopoietic lineage (Nagata et al., 1996; Hafizi et al., 2006). AML is characterized by abnormal proliferation and survival of myeloid progenitor and precursor cells and a premature block in myeloid differentiation (Lu et al., 1999). It accounts for roughly 70-80% of all adult acute leukemias and 20% of all childhood acute leukemias (Löwenberg et al., 1999). Despite aggressive therapies, AML remains difficult to treat, and many patients will die as a consequence of treatment failure or complications from either treatment-related toxicities or impaired normal hematopoiesis (Chen et al., 2010). The majority of AML respond to initial treatment; however relapse is common indicating resistance of malignant cells to chemotherapy (Meenaghan et al., 2012). For AML patients who relapse or have resistant disease, therapeutic options are limited. Therefore, the need for effective yet better tolerated new therapies is needed.

MicroRNAs (miRNAs) are regulatory RNAs. They are a ~22 nucleotides in length and serve to regulate post

transcriptional expression of target genes (He and Hannon, 2004). They mediate fundamental cellular processes such as proliferation, differentiation and apoptosis and are actively involved in carcinogenesis (He and Hannon, 2004; Xiao and Rajewski, 2009). MicroRNA-155 (MiR-155) is one of the most frequently overexpressed miRNAs in solid as well as hematological malignancies. Aberrant expression of miR-155 has been found to be associated with various types of hematological malignancies, such as Hodgkin's lymphoma, diffuse large B-cell lymphoma (DLBCL), acute myeloid leukemia (AML) and chronic lymphoid leukemia (Calin and Croce, 2006; Cui et al., 2014), suggesting its oncogenic role in their pathogenesis. Overexpression of miR-155 has also been found to be associated with the more aggressive and poorer prognosis type of CLL (Cui et al., 2014). In AML, high expression of miR-155 independently predicts poor outcome in cytogenetically normal patients and is associated with high-risk FLT3 internal tandem duplication (ITD) mutations (Whitman et al., 2010; Marcucci et al., 2013). Ectopic expression of miR-155 in hematopoietic progenitors can induce either a myeloproliferative disorder or an aggressive B-cell leukemia in mice, supporting a leukemogenic role of miR-155 (O'Connell et al., 2008; Costinean et al., 2009). Babar (Babar et al., 2012) has shown that overexpression of miR-155 in lymphoid tissues resulted in disseminated lymphoma characterized by a clonal, transplantable pre-B-cell population of neoplastic lymphocytes. Withdrawal of miR-155 in mice with established disease resulted in rapid regression of lymphadenopathy. Systemic delivery of antisense peptide nucleic acids encapsulated in unique polymer nanoparticles inhibited miR-155 and slowed the growth of these pre-B-cell tumors *in vivo* (Babar et al., 2012).

Different mechanisms have been postulated for the miR-155-mediated pathogenesis of hematological malignancies. miR-155 is upregulated by the transcription factor FoxP3 and is critical for T regulatory cell function (Kohlhaas et al., 2009). Mice overexpressing miR-155 in the B-cell lineage results in preleukemic pre-B-cell proliferation in the spleen and bone marrow, followed later in life by B-cell malignancy (Costinean et al., 2006). miR-155 represses genes encoding DNA damage response proteins (Tili et al., 2011). However, the molecular mechanism of how miR-155 functions in cancer has not been defined.

PUMA is a BH3-only member of the Bcl-2 family and a target of p53-mediated apoptosis (Yu et al., 2003). It activates an apoptotic cascade by facilitating Bax activation, causing cytochrome C release from the mitochondria, caspase-3 activation and DNA fragmentation (Kim et al., 2009). Zhang et al. (2010a,b) has found that miR-221/222 inhibited cell apoptosis and decreased tumor growth in xenograft model by targeting pro-apoptotic gene PUMA in human glioma cells. Cazanave et al. found enforced miR-296-5p levels efficiently reduced PUMA protein expression in Huh-7 cells, while antagonism of miR-296-5p function increased PUMA cellular levels (Cazanave et al., 2011). Adlakha et al. found that miR-128 induces apoptosis via induction of PUMA, and pretreatment with PUMA and Bak siRNAs abolished miR-128-induced apoptosis of HCT116 cells (Adlakha et al., 2013). Ghorpade (Ghorpade et al., 2012) found that enforced expression of miR-155 resulted in augmented expression of PUMA transcripts in macrophages. Importantly, repression of *M. bovis* BCG-triggered miR-155 expression, either by miR-155 specific small interfering RNA (siRNA) or by anti-miR-155 (anti-miR-155 oligonucleotide) reduced the transcript levels of PUMA, suggesting that PUMA might be regulated by miR-155.

Slug is a zinc finger transcriptional repressor of the Slug/Snail family that promotes carcinoma cell invasion, stemness, and survival (Nieto et al., 2002). Numerous studies have reported that Slug is a target of miRNAs (Qiu et al., 2013; Liang et al., 2013; Tominaga et al., 2013; Osaka et al., 2014; Chang et al., 2016; Yang et al., 2016). In addition, Slug is a strong inhibitor of PUMA, targeting slug induced apoptosis by PUMA upregulation (Jiang et al., 2016).

The purpose of this study was to investigate the potential role of targeting miR-155 on proliferation and apoptosis of HL-60 cells *in vitro* and *in vivo*, and explore its mechanisms.We found that knockdown of miR-155 inhibits proliferation and induces apoptosis of HL-60 cells by Slug/PUMA signal.

Materials and methods

Cell line and culture

The HL-60 cell line was purchased from the Insitute of Biochemistry and Cell Biology (Shanghai, China). The cell line was maintained in RPMI 1640 (Life, Technologies), supplemented with antibiotics (100 U/mL penicillin and100 U/mL streptomycin), 3mmol/L L-glutamine and 10% (v/v) fetal bovine serum (Wisent, Montréal, PQ).

Stable anti-miR-155 transfection

anti-miR-155 and scramble control were purchased from Ambion (Applied Biosystems, Shanghai, China). HL-60 cells were transfected with anti-miR-155 or scramble control overnight according to the manufacturers' instructions. After 72hr, the cells selected with 1 μg/ml G418 for 14 days. Total RNA was extracted and quantitative reverse transcription polymerase chain reaction (qRT-PCR) was performed to verify the levels of miR-155.

Stable PUMA siRNA transfection

HL-60 cells were transfected with the PUMA siRNA

or control siRNA expression plasmid using Lipofectamine2000 reagent according to manufacturer's instructions. After transfection for 48 h, the cells were selected with 1 μg/ml G418 for 14 days. The levels of PUMA proteins in the transfected cells were verified by Western blot.

Transient Slug cDNA plasmid transfection

The stable anti-miR-155 transfected HL-60 cells (anti-miR-155/HL-60) were transfected with the Slug cDNA expression plasmid (Gifted by Dr Chen) (pcDNA3.1 as control plasmid) using Lipofectamine2000 reagent according to manufacturer's instructions. The levels of Slug and PUMA proteins in the transfected cells were verified by Western blot.

Western blotting

At every experimental end point, cells in different groups were lysed using Cellytic™ M cell lysis reagent (Sigma) that contained 1 mM NaF, 1 mM PMSF and 0.4 mM protease inhibitors cocktail (Roche, Hangzhou, China). Protein concentration was measured using the protein assay from Bio-Rad (Hercules, Guangzhou, China). Equal amounts of protein (40 μg) were subjected to SDS-PAGE on an 10% acrylamide gel. After electrophoresis, the proteins were electrotransferred to nitrocellulose membranes (Amersham) and blocked with 5% nonfat dry milk, the membranes were incubated with anti-Slug, PUMA, Mcl-1, Bim, Bid, Bad, Bcl-Xl, Bcl-2, caspase-3, cytochrome c and anti-β-actin antibodies (Santa Cruz, Shanghai, China) at 4°C overnight followed by incubation with horseradish peroxidase-conjugated goat anti-rabbit serum (BD Biosciences) and rabbit anti-goat serum (DAKO), and visualized via chemiluminescence detection (Amersham Biosciences). Representative blots are shown from 3 independent experiments.

qRT-PCR analysis

Quantitive RT-PCR (qRT-PCR) analysis was used to determine the relative expression levels of miR-155 in HL-60 cells. At every experimental end point, cells were collected and washed twice with ice-cold PBS and lysed with QIAzol reagent to isolate total RNA. miRNA was isolated using an miRNeasy kit (Qiagen) from the total RNA above.The cDNA was synthesized from total RNA using a TaqMan miRNA Reverse transcription kit (Applied Biosystems, USA) as the manufacture's instruction.

Subsequently, quantitive PCR was performed using primers and materials from Applied Biosystems. PCR cycle threshold (Ct) values were recorded for each target gene and for normalization controls and were averaged across three independent runs. All reactions were performed in triplicate, and the results were analyzed using the $2^{-\Delta\Delta Ct}$ or $2^{-\Delta Ct}$ method.

Cell proliferation assays

Cell growth was evaluated by BrdU proliferation assay. Briefly, cells (5.0×10^3) at every experimental end point were plated onto a 24-well plate and allowed to attach for 24 h. The culture medium was then replaced with fresh medium. The cells were then permitted to incorporate with BrdU (50 μM) for 1.5 hours. Cells were then washed with PBS, trypsinized, and washed again. BrdU staining was performed according to an adaptation of the manufacturer's protocol. BrdU-incorporation was detected according to the manufacturer's protocol for flow cytometry analysis on a FACScan instrument.

MTT assay for cell viability

At every experimental end point, cells from each group were collected and plated in 96-well plates at a density of 1.0×10^4 cells/well for MTT assay. The absorbance was measured at 570 nm. Each assay was performed in triplicate. Cell growth (mean absorbance ± standard deviation) was plotted versus time.

Clonogenic assay

At every experimental end point, cells were seeded in 6-well plates at a density of 600 cells/well and incubated for 2 weeks at 37°C in a humidified atmosphere of 5% CO_2. The colonies were fixed with in 4% paraformaldehyde at room temperature for 20 min, stained with 0.1% crystal violet for 10 min, and finally, positive colony formation (more than 50 cells/colony) was counted and colony formation rate was calculated.

In vitro apoptosis assay

At every experimental end point, the cells were harvested and washed twice with cold PBS, then the cells were stained with Annexin V-FITC and 10 μl propidium iodide (PI) using the Annexin V-FITC Apoptosis Detection Kit (KEYGEN, Nanjing, China). The percentage of apoptotic cells was detected using a FACSCalibur Flow cytometer (BD, San Jose, CA, USA). All analyses were performed in triplicate.

In vitro TUNEL staining

The terminal deoxyribonucleotidyl transferase mediated dUTP nick end labeling (TUNEL) assay was performed to detect apoptosis using the In Situ Cell Death Detection Kit (Roche Applied Science, Shanghai, China) according to the manufacturer's instruction. Briefly, after the FACS, the cells were fixed in 4% paraformaldehyde for 30 min and then washed with PBS for 1 min. The coverslips were rountinely incubated with a permeabilization solution at 4°C. After 5 min, coverslips were washed with PBS and then incubated with TUNEL reaction mixture for 1 h at 37°C in a humidified chamber. Incubating the coverslips in label

solution was as the negative control. Incubating the coverslips with DNase I recombinant was the positive control. After incubating the coverslips with DNase I or label solution for 2 hs, the coverslips were then incubated with Hoechst 33342 (10 μg/ml) for 10 min at room tempreture in a humidified dark chamber. Coverslips were then washed three times with PBS and mounted with mounting solution (Sigma) after 3 times washing with PBS. Fluorescence microscope was then used to analyze TUNEL staining in mounting medium. The percentage of positively stained cells was determined by counting all cells per view until reaching ~100 cells per sample using a confocal microscope.

HL-60 cell xenograft studies

Four-week-old male mice were purchased from Jackson Laboratory (Bar Harbor, ME). For each mouse, 3×10^6 anti-miR-155/HL-60 or control/HL-60 cells in 100 μl PBS were subcutaneously inoculated in the left and right flank areas (N=6). The mice were observed over 8 weeks for tumor formation.The mice were sacrificed, and tumors were dissected after 8 weeks. The tumors were excised. Half of each tumor was fixed in 4% buffered formaldehyde, paraffin-embedded and processed for histological examination, while the second half was frozen in liquid nitrogen and stored in -80°C for immunoblot analysis, qRT- PCR and TUNEL assay.

In vivo TUNEL staining

Tissue sections were prepared and treated according to manufacturer's recommendations (TACS XL; Guangzhou, China).

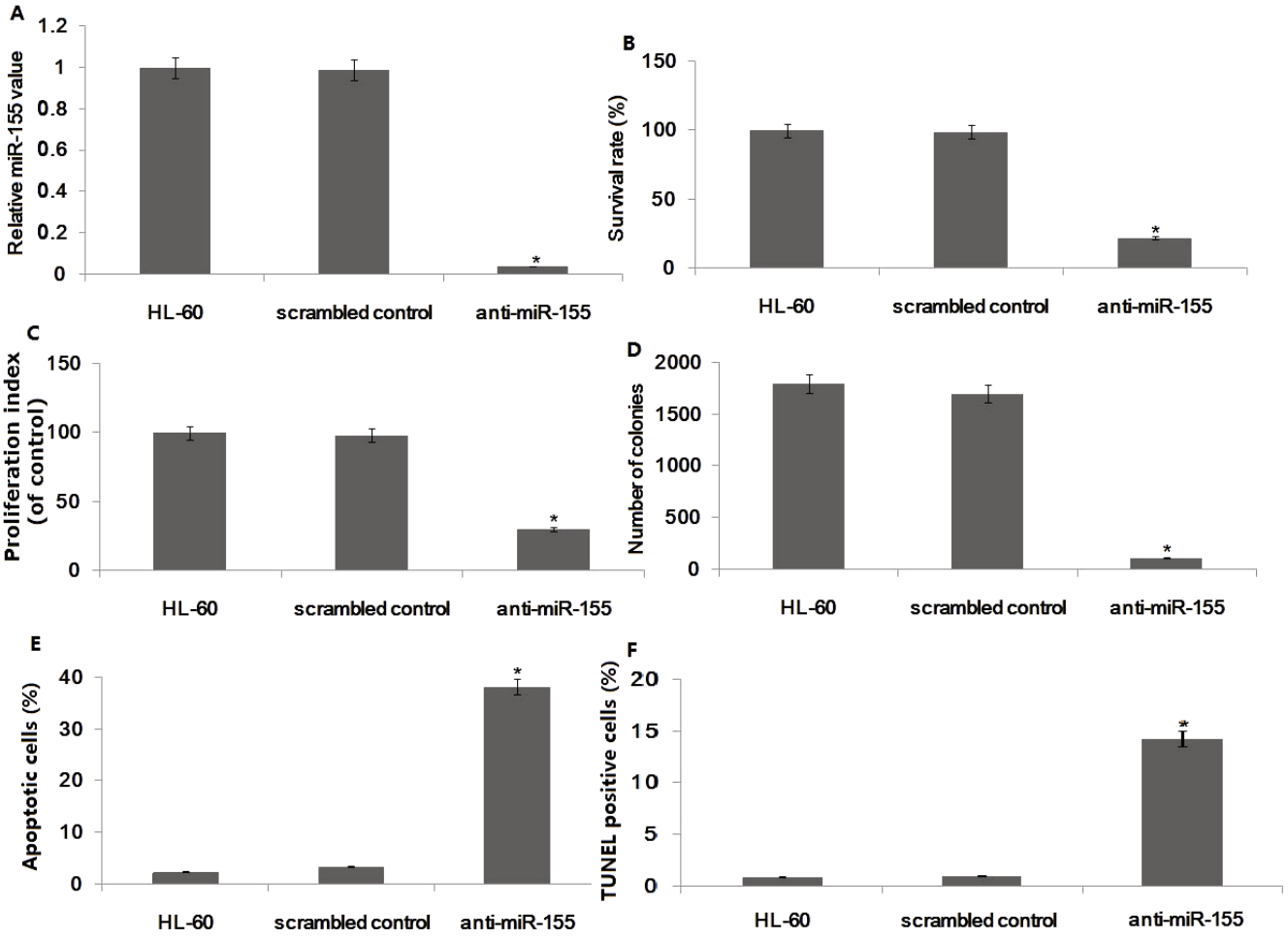

Fig. 1. Targeting miR-155 induces apoptosis and inhibits growth and colony formation of HL-60 cells *in vitro*. HL-60 cells were transfected with anti-miR-155. **A.** miR-155 mRNA expression was detected by qRT-PCR assay. **B.** Cell viability by MTT assay. **C.** Cell proliferation by BrdUrd cell proliferation assay. **D.** Cell growth by colony formation assay. **E.** Cell apoptosis was detected by FCM. **F.** Cell apoptosis was detected by TUNEL assay. The data are shown as the mean ± SD. The experiments were all repeated at least 3 times to confirm the reproducibility of the results. *p<0.05 versus the control.

Statistical analysis

All data are presented as mean ± S.E. Statistical analyses were performed using SPSS.21 Software. The significance was determined by two tailed Student's t test or one-way analysis of variance with Bonferroni post tests where applicable. Experiments were performed in triplicate. p value less than 0.05 was considered statistically significant.

Results

Targeting miR-155 inhibits growth of HL-60 cells

The effect of miR-155 downexpression on tumor HL-60 cell growth was investigated. miR-155 expression levels could be decreased up to 24-fold in the anti-miR-155-transfected HL-60 cells compared with scrambled control-transfected cells (Fig. 1A). miR-155-downexpressing cells led to decreased viability by MTT assay (Fig. 1B). To confirm cell growth inhibition, we also conducted the cell proliferation assay using the BrdU labeling and Detection Kit. We found similar results as MTT assay using this method (Fig. 1C). Clonogenic survival assay also showed a 10-fold reduction of colony numbers in anti-miR-155-infected cells (Fig. 1D). Next, we examined whether the inhibition of cell growth was also accompanied by the induction of apoptosis induced by anti-miR-155. Annexin V/PI staining and TUNEL were employed to investigate the degree of apoptosis induced by anti-miR-155.

Targeting miRNA-155 induces apoptosis of HL-60 cells

As shown in Fig. 1E, following anti-miR-155 transfection, HL-60 cells showed many apoptotic cells by Annexin V/PI staining. The number of TUNEL-positive cells also increased with the anti-miR-155 transfection for 72h (Fig. 1F).

Targeting miR-155 induces PUMA in HL-60 cells

We first investigated the effects of miR-155 sliencing on PUMA expression in HL-60 cells. Targeting miR-155 led to rapid increase of PUMA protein within 24 h of transfection and reached the peak at 72 h (Fig. 2A). Interestingly, the expression of Bcl-2 family members, such as Mcl-1, Bim, Bid, Bad, Bcl-xL and Bcl-2 remained unchanged by 72h (Fig. 2). Furthermore, the caspase-3 and cytochrome c downstream of PUMA was also activated by miR-155 sliencing (Fig. 2), suggesting that miR-155 sliencing selectively induced PUMA protein expression.

PUMA is essential for anti-miR-155 induced apoptosis in HL-60 cells

Next we determined the role of PUMA in anti-miR-155-induced apoptosis and growth inhibition. PUMA knockdown with siRNA led to reduced apoptosis in HL-60 cells following anti-miR-155 transfection (Fig. 3A,B) with little or no activation of caspases-3 and cytochrome c release at 72 h of anti-miR-155 transfection (Fig. 3E). In addition, PUMA siRNA transfection reversed anti-miR-155 induced growth inhibition (Fig. 3C,D). Collectively, these results demonstrate an essential role of PUMA and the mitochondrial pathway in anti-miR-155-induced apoptosis and growth inhibition in HL-60 cells.

Slug-dependent induction of PUMA by miR-155

HL-60 cells were transfected with anti-miR-155, Slug protein expression was significantly decreased by

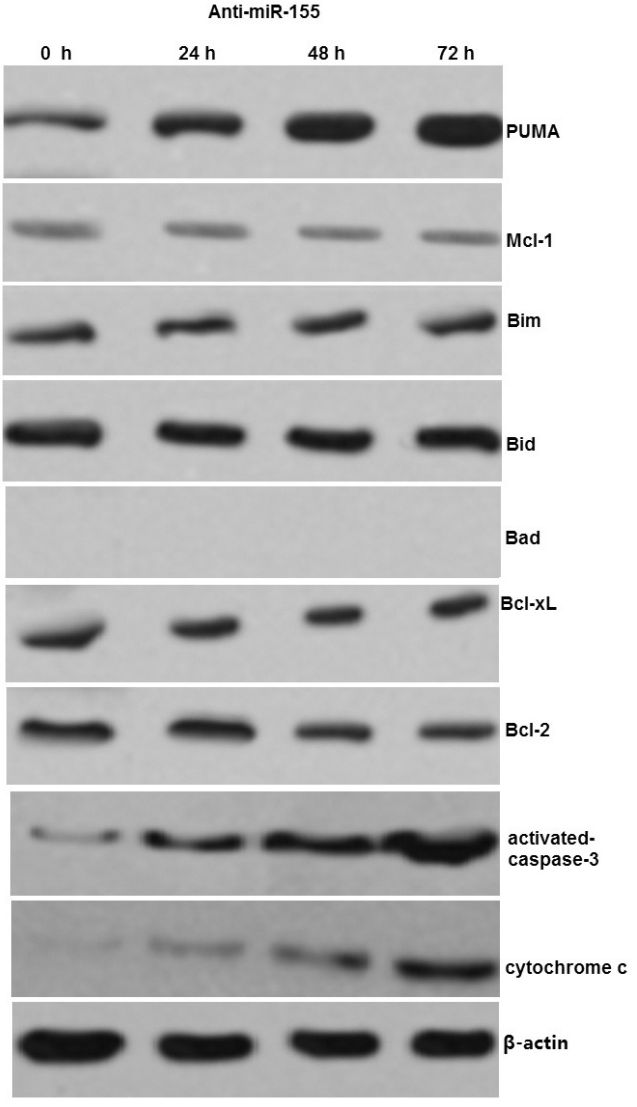

Fig. 2. Targeting miR-155 induces PUMA expression in HL-60 cells. Western blot analysis of the expression of Bcl-2 family members at indicated time points in HL-60 cells transfected with anti-miR-155.

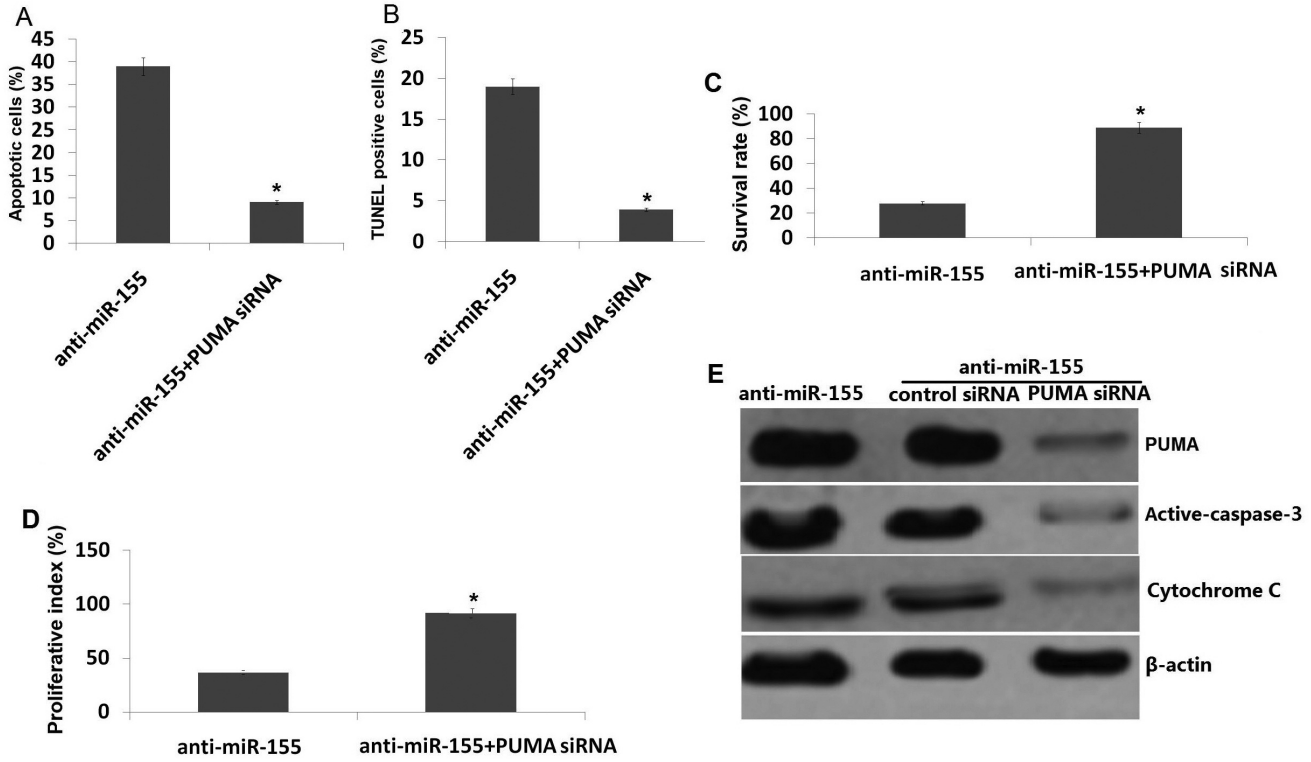

Fig. 3. Targeting PUMA inhibited anti-miR-155-induced apoptosis in HL-60 cells. HL-60 cells were transfected with anti-miR-155 or/and PUMA siRNA. **A.** Cell apoptosis was detected by FCM. **B.** Cell apoptosis was detected by TUNEL assay. **C.** Cell proliferation by MTT assay. **D.** Cell proliferation by BrdUrd cell proliferation assay. **E.** Western blot analysis of the expression of PUMA,caspase-3 and cytochrome C in HL-60 cells transfected with anti-miR-155/PUMA siRNA.The data are shown as the mean ± SD. The experiments were all repeated at least 3 times to confirm the reproducibility of the results. *p<0.05 versus the control.

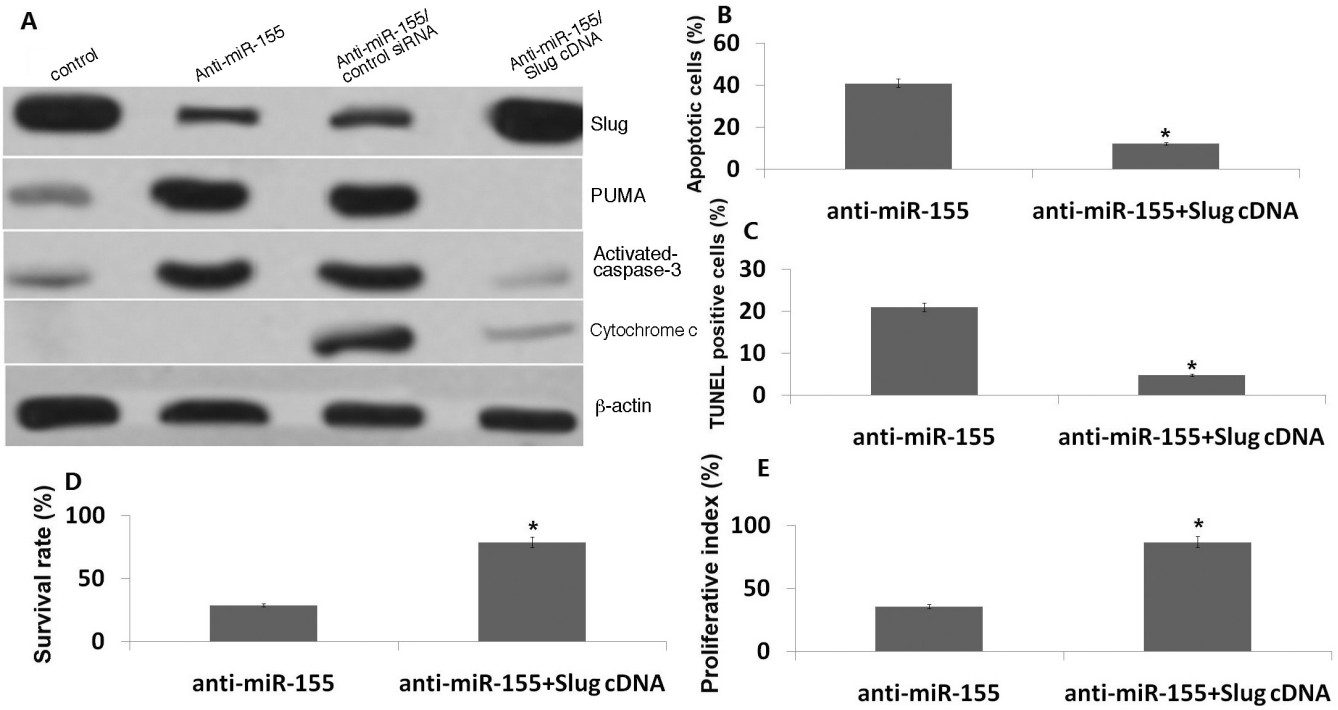

Fig. 4. Slug overexpression inhibited anti-miR-155-induced apoptosis in HL-60 cells. HL-60 cells were transfected with anti-miR-155 or/and Slug cDNA. **A.** Western blot analysis of the expression of Slug, PUMA, caspase-3 and cytochrome C in HL-60 cells transfected with anti-miR-155/Slug cDNA. **B.** Cell apoptosis was detected by FCM. **C.** Cell apoptosis was detected by TUNEL assay. **D.** Cell proliferation by MTT assay. **E.** Cell proliferation by BrdUrd cell proliferation assay. The data are shown as the mean ± SD. The experiments were all repeated at least 3 times to confirm the reproducibility of the results. *p<0.05 versus the control.

western blot assay (Fig. 4A). We transfected Slug cDNA into anti-miR-155 transfected HL-60 cells, and found PUMA, caspase-3 and cytochrome C release was significantly decreased (Fig. 4A). In addition, Slug cDNA transfection inhibited apoptosis in anti-miR-155 transfected HL-60 cells (Fig. 4B,C). Morever, Slug cDNA transfection reversed anti-miR-155 induced growth inhibition (Fig. 4D,E).

Targeting miR-155 inhibits the growth of HL-60 cells xenografted in mice

Having validated our cell model *in vitro*, we next evaluated the *in vivo* effect of miR-155 sliencing on HL-60 tumor xenograft growth. Stably anti-miR-155 and control transfected HL-60 cell suspensions were injected s.c. into the flanks of 6-week-old immunodeficient mice, and tumor growth was evaluated and registered periodically, to plot tumor growth curves. Tumors arose ~2 weeks after subcutaneous administration, and tumorigenicity studies were terminated at 6 weeks after cell implantation. Our results demonstrate anti-miR-155 transfection suppressed the growth of HL-60 tumors by 80% compared to control transfected xenografts, from the 5 weeks after implantation until the end of the experiment at 6 weeks (Fig. 5A).

We next evaluated the effect of targeting miR-155 on apoptosis and proliferation of HL-60 xenografts in mice. In stably anti-miR-155 transfected xenografts, miR-155 (Fig. 5B) and Slug (Fig. 5C) were significantly decreased, whereas PUMA, caspase-3 and cytochrome c release was significantly increased (Fig. 5C). As expected, the frequency of TUNEL-positive cells was increased in anti-miR-155 versus control xenograft tumoral tissue ($p<0.01$, Fig. 5D).

Discussion

The data presented here indicate that targeting miR-155 in AML cell HL-60 lines inhibited cell growth and induced apoptosis.The proapoptotic and antiproliferative effect of anti-miR-155 in HL-60 cell lines was observed after 72 hours of transfection. These results indicate that anti-miR-155-dependent cell antiproliferation effects ere the result of apoptosis and likely to contribute to the tumor suppressor activity of anti-miR-155. The tumor suppressor effect of anti-miR-155 in HL-60 cells was further demonstrated *in vivo*.

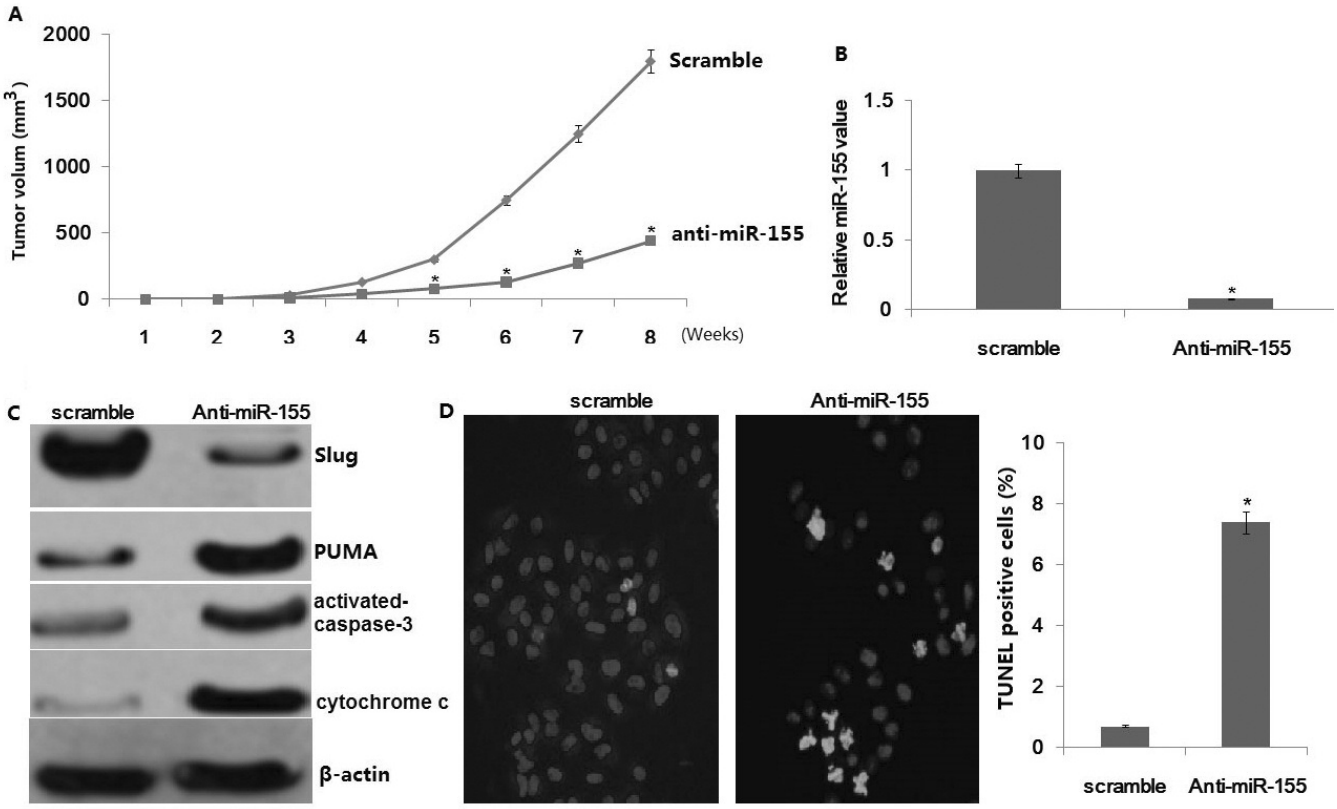

Fig. 5. *In vivo* antitumor activity of anti-miR-155 against s.c. xenografted tumors of HL-60 cells in mice. **A.** Subcutaneous tumors were seeded in immunodeficient mice using HL-60 cells, as described in the Materials and methods section. **B.** miR-155 mRNA was detected by qRT-PCR. **C.** Slug, PUMA, caspase-3 and cytochrome C expression was detected by western blot assay. **D.** TUNEL staining in the tumors. Significant differences between the anti-miR-155 groups and scramble group are indicated by *P<0.01. × 400

To characterize the anti-miR-155 tumor suppressor function in leukemia and identify the pathways regulated by miR-155, we analyzed the expression changes in the HL-60 cell line after targeting miR-155. Pro-apoptotic PUMA (p53 upregulated modulator of apoptosis) is a potent pro-apoptotic protein belonging to the Bcl-2 protein family. PUMA binds to the pro-survival proteins Bcl-2, Bcl-X_L, and Mcl-1, thereby allowing Bax and Bak to promote apoptosis (Ming et al., 2006). Liu et al. (2014) found that up-regulation of PUMA sensitized Cyt-induced apoptosis in HL-60 cells. Some studies have reported that activation of both extrinsic and intrinsic apoptotic pathways was involved in LG-induced AML cell apoptosis, accompanied by dissipation of mitochondrial membrane potential, downregulation of anti-apoptotic proteins (Bcl-2, Mcl-1, and Bcl-xL) and upregulation of pro-apoptotic protein PUMA (Teng et al., 2014). Zhang et al has recently reported that PUMA was the essential and major regulator of AML cell survival (Zhang et al., 2010a,b). Our findings showed that targeting miR-155 inhibited cell proliferation and induced apoptosis, followed by PUMA upregulation. However, knockdown of PUMA by siRNA transfection inhibited anti-miR-155-induced apoptosis and proliferation inhibition in HL-60 cells, suggesting that the identification of PUMA as a miR-155 target gene may explain why targeting miR-155 suppressed the proliferation and induced apoptosis of HL-60 cells.

Also the apoptosis provoked by anti-miR-155 requires activation of PUMA, but how anti-miR-155 regulated PUMA has remained unknown. Slug is a zinc finger transcriptional repressor that promotes carcinoma cell invasion, stemness, survival and inhibits apoptosis. It is well known that Slug negatively regulated PUMA expression (Jiang et al., 2016). In this study, we found that anti-miR-155 inhibited Slug expression in the HL-60 cells. However, overexpression of Slug by Slug cDNA transfection reversed anti-miR-155-induced PUMA expression and reversed anti-miR-155 induced growth inhibition and apoptosis. We therefore suggested that targeting miR-155 exhibits significant *in vivo* and *in vitro* antileukemic activities in AML through a novel mechanism resulting in inhibition of Slug expression and inducing PUMA expression.

Conclusion

Our study highlights targeting miR-155 induced Slug-dependent PUMA expression, thereby reducing cell viability and enhancing apoptosis in the HL-60 cells. We therefore suggested that miR-155 could be an effect target for acute myeloid leukemia therapeutics.

Acknowledgements. LH and RYG designed the study and write the manuscript. WSL, LJF and ZW performed most of the experiments. WZY and GLZ performed the western blot assay. RYG performed the RT-PCR. LJF performed the transfection. RYG analyzed the data and performed statistical analysis. All of them read and approved the final manuscript.

References

Adlakha Y.K. and Saini N. (2013). miR-128 exerts pro-apoptotic effect in a p53 transcription-dependent and -independent manner via PUMA-Bak axis. Cell Death Dis. 4,e542.

Babar I.A., Cheng C.J., Booth C.J., Liang X., Weidhaas J.B., Saltzman W.M. and Slack F.J. (2012). Nanoparticle-based therapy in an *in vivo* microRNA-155 (miR-155)-dependent mouse model of lymphoma. Proc. Natl. Acad. Sci. USA 109, E1695-1704.

Calin G.A. and Croce C.M. (2006). MicroRNA signatures in human cancers. Nat. Rev. Cancer 6, 857-866.

Cazanave S.C., Mott J.L., Elmi N.A., Bronk S.F., Masuoka H.C., Charlton M.R. and Gores G.J. (2011). A role for miR-296 in the regulation of lipoapoptosis by targeting PUMA. J. Lipid. Res. 52, 1517-1525.

Chang C.W., Yu J.C., Hsieh Y.H., Yao C.C., Chao J.I., Chen P.M., Hsieh H.Y., Hsiung C.N., Chu H.W. and Shen C.Y. (2016). MicroRNA-30a increases tight junction protein expression to suppress the EMT and metastasis by targeting Slug in breast cancer. Oncotarget 24, 329-338

Chen J., Odenike O. and Rowley J.D. (2010). Leukaemogenesis: more than mutant genes. Nat. Rev. Cancer 10, 23-36.

Costinean S., Zanesi N. and Pekarsky Y. (2006). Pre-B cell proliferation and lymphoblastic leukemia/high-grade lymphoma in Eμ-miR155 transgenic mice. Proc. Natl. Acad. Sci. USA 103, 7024-7029.

Cui B., Chen L., Zhang S., Mraz M., Fecteau J.F., Yu J., Ghia E.M., Zhang L., Bao L., Rassenti L.Z., Messer K., Calin G.A., Croce C.M. and Kipps T.J. (2014). MicroRNA-155 influences B-cell receptor signaling and associates with aggressive disease in chronic lymphocytic leukemia. Blood 124,546-554.

Ghorpade D.S., Leyland R., Kurowska-Stolarska M., Patil S.A. and Balaji K.N. (2012). MicroRNA-155 is required for Mycobacterium bovis BCG-mediated apoptosis of macrophages. Mol. Cell Biol. 32, 2239-2253.

Hafizi S., Dahlbäck B. Gas6 and protein S. (2006). Vitamin K-dependent ligands for the Axl receptor tyrosine kinase subfamily. FEBS J. 273, 5231-5244.

He L. and Hannon G.J. (2004). MicroRNAs: small RNAs with a big role in gene regulation. Nat. Rev. Genet. 5, 522-531.

Jiang F., Zhou L., Wei C., Zhao W. and Yu D. (2016). Slug inhibition increases radiosensitivity of oral squamous cell carcinoma cells by upregulating PUMA. Int. J. Oncol. 49, 709-719

Kim H., Tu H.C., Ren D., Takeuchi O., Jeffers J.R., Zambetti G.P., Hsieh J.J. and Cheng E.H. (2009).Stepwise activation of BAX and BAK by tBID, BIM, and PUMA initiates mitochondrial apoptosis. Mol. Cell 36, 487-499.

Kohlhaas S., Garden O.A., Scudamore C., Turner M., Okkenhaug K. and Vigorito E. (2009). Cutting edge: the Foxp3 target miR-155 contributes to the development of regulatory T cells1. J. Immunol. 182, 2578-2582.

Liang Y.J., Wang Q.Y., Zhou C.X., Yin Q.Q., He M., Yu X.T., Cao D.X., Chen G.Q., He J.R. and Zhao Q. (2013). MiR-124 targets Slug to regulate epithelial-mesenchymal transition and metastasis of breast cancer. Carcinogenesis 34, 713-722.

Liu G.J., Pan G.J., Wang J., Wang L.N., Xu Y. and Tang Y. (2014). Knockdown of ERK/Slug signals sensitizes HL-60 Leukemia cells to Cytarabine via upregulation of PUMA. Eur. Rev. Med. Pharmacol. Sci. 18, 3802-3809.

Löwenberg B., Downing J.R., and Burnett A. (1999). Acute myeloid

leukemia. N. Engl. J. Med. 341, 1051-1062.

Lu Q., Gore M. and Zhang Q. (1999). Tyro-3 family receptors are essential regulators of mammalian spermatogenesis. Nature 398, 723-728.

Marcucci G., Maharry K.S., Metzeler K.H., Volinia S., Wu Y.Z., Mrózek K., Nicolet D., Kohlschmidt J., Whitman S.P., Mendler J.H., Schwind S., Becker H., Eisfeld A.K., Carroll A.J., Powell B.L., Kolitz J.E., Garzon R., Caligiuri M.A., Stone R.M. and Bloomfield C.D. (2013). Clinical role of microRNAs in cytogenetically normal acute myeloid leukemia: miR-155 upregulation independently identifies high-risk patients. J. Clin. Oncol. 31, 2086-2093.

Meenaghan T., Dowling M. and Kelly M. (2012). Acute leukaemia: making sense of a complex blood cancer. Br. J. Nurs. 21, 76, 78-83.

Ming L., Wang P., Bank A., Yu J. and Zhang L. (2006). PUMA Dissociates Bax and Bcl-X(L) to induce apoptosis in colon cancer cells. J. Biol. Chem. 281, 16034-16042.

Nagata K., Ohashi K. and Nakano T. (1996). Identification of the product of growth arrest-specific gene 6 as a common ligand for Axl, Sky, and Mer receptor tyrosine kinases. J. Biol. Chem. 271, 30022-30027.

Nieto M.A. (2002). The snail superfamily of zinc-finger transcription factors. Nat. Rev. Mol. Cell Biol. 3, 155-166.

O'Connell R.M., Rao D.S., Chaudhuri A.A., Boldin M.P., Taganov K.D., Nicoll J., Paquette R.L. and Baltimore D. (2008). Sustained expression of microRNA-155 in hematopoietic stem cells causes a myeloproliferative disorder. J. Exp. Med. 205, 585-594.

Osaka E., Yang X., Shen J.K., Yang P., Feng Y., Mankin H.J., Hornicek F.J. and Duan Z. (2014). MicroRNA-1 (miR-1) inhibits chordoma cell migration and invasion by targeting slug. J. Orthop. Res. 32,1075-1082.

Qiu Y.H., Wei Y.P., Shen N.J., Wang Z.C., Kan T., Yu W.L., Yi B. and Zhang Y.J. (2013).miR-204 inhibits epithelial to mesenchymal transition by targeting slug in intrahepatic cholangiocarcinoma cells. Cell Physiol. Biochem. 32, 1331-1341.

Teng C.L., Han S.M., Wu W.C., Hsueh C.M., Tsai J.R., Hwang W.L. and Hsu S.L. (2014). Mechanistic aspects of lauryl gallate-induced differentiation and apoptosis in human acute myeloid leukemia cells. Food Chem. Toxicol. 71, 197-206.

Tili E., Michaille J.J. and Wernicke D. (2011). Mutator activity induced by microRNA-155 (miR-155) links inflammation and cancer. Proc. Natl. Acad. Sci. USA 108, 4908-4913.

Tominaga E., Yuasa K., Shimazaki S. and Hijikata T. (2013). MicroRNA-1 targets Slug and endows lung cancer A549 cells with epithelial and anti-tumorigenic properties. Exp. Cell Res. 319, 77-88.

Whitman S.P., Maharry K., Radmacher M.D., Becker H., Mrózek K., Margeson D., Holland K.B., Wu Y.Z., Schwind S., Metzeler K.H., Wen J., Baer M.R., Powell B.L., Carter T.H., Kolitz J.E., Wetzler M., Moore J.O., Stone R.M., Carroll A.J., Larson R.A., Caligiuri M.A., Marcucci G. and Bloomfield C.D. (2010). FLT3 internal tandem duplication associates with adverse outcome and gene- and microRNA-expression signatures in patients 60 years of age or older with primary cytogenetically normal acute myeloid leukemia: a Cancer and Leukemia Group B study. Blood 116, 3622-3626.

Xiao C. and Rajewsky K. (2009). MicroRNA control in the immune system: basic principles. Cell 136, 26-36.

Yang L., Liang H., Wang Y., Gao S., Yin K., Liu Z., Zheng X., Lv Y., Wang L., Zhang C.Y., Chen X., Xu G., Zhang W. and Zou X. (2016). MiRNA-203 suppresses tumor cell proliferation, migration and invasion by targetingSlug in gastric cancer. Protein Cell 7, 383-387.

Yu J., Wang Z., Kinzler K.W., Vogelstein B. and Zhang L. (2003). PUMA mediates the apoptotic response to p53 in colorectal cancer cells. Proc. Natl. Acad. Sci. USA 100, 1931-1936.

Zhang C.Z., Zhang J.X., Zhang A.L., Shi Z.D., Han L., Jia Z.F., Yang W.D., Wang G.X., Jiang T., You Y.P., Pu P.Y., Cheng J.Q. and Kang C.S. (2010a). MiR-221 and miR-222 target PUMA to induce cell survival in glioblastoma. Mol. Cancer 9, 229.

Zhang W., Konopleva M., Burks J.K., Dywer K.C., Schober W.D., Yang J.Y., McQueen T.J., Hung M.C. and Andreeff M. (2010b). Blockade of mitogen-activated protein kinase/extracellular signal-regulated kinase kinase and murine double minute synergistically induces Apoptosis in acute myeloid leukemia via BH3-only proteins Puma and Bim. Cancer Res. 70, 2424-2434.

Accepted October 27, 2016